u	is the bubble velocity;
R_0	is the bubble radius;
ε	is the porosity;
ν	is the kinematic viscosity;
σ	is the surface-tension coefficient;
g	is the acceleration due to gravity;
R	is the radius of packing grain, d = 2R;
u_3	is the piston velocity;
Fr, Eö	are the Froude and Eötvös numbers, respectively;
ρ_2, ρ_1	are the densities of liquid and gas, respectively;
L	is the distance between pistons;
D	is the column diameter;
S_{sp}	is the specific surface of the packing;
φ_l	is the local gas percentage at the side surface of grains;
β	is the volumetric gas percentage.

LITERATURE CITED

1. V. A. Kirillov, B. L. Ogarkov, and V. G. Voronov, Inzh.-Fiz. Zh., 31, No. 3 (1976).
2. Advances in the Field of Heat Exchange [Russian translation], Mir, Moscow (1970), p. 7.
3. Investigation of the Turbulent Flow of Two-Phase Media [in Russian], Nauka, Novosibirsk (1970).
4. M. A. Kasamanyan, Author's Abstract of Candidate's Dissertation, Novosibirsk (1974).
5. J. S. Bendat and A. G. Piersol, Random Data: Analysis and Measurement Procedures, Wiley (1971).
6. E. G. Dudnikov et al., Mathematical Simulators of Chemical Technology Systems [in Russian], Khimiya, Leningrad (1970).
7. M. É. Aérov and O. M. Todes, Hydraulic and Thermal Principles of the Operation of Apparatus with Fixed Granular Layers and Fluidized Beds [in Russian], Khimiya, Leningrad (1968).
8. Moisis and Griffis, Teploperedacha, Ser. C, 84, No. 1 (1962).

EFFECTIVE DENSITY OF A FLUIDIZED BED

Yu. I. Zinov'ev

UDC (631.358.45+66.096.5):001.5

Pressure coefficients have been determined for a fluidizing agent flowing around a sphere. A method is presented for calculating the integral aerodynamic force; formulas are given for the variation in the apparent aerodynamic density and effective density for a fluidized bed.

If a fluidized bed is to be used as a means of separating materials by density, one needs to know the effective density corresponding to the actual upthrust on an immersed body. Not much is known about the exact origin of this force or the factors that affect it. The effects of a fluidized bed on an immersed sphere have been equated to those of an Archimedean liquid. The density of the pseudofluid has been taken as that of the mass of the grains of solid per unit volume of the suspension. The observed forces differ from the Archimedean value in both senses, which is due to the pressure exerted by the body of grains in the stagnant zone [1, 2, 12] and also to rising currents of the solid [3] or of the solid and fluidizing agent together [14]. It has also been claimed [8, 14] that the force increases with the fluidization number and as the size of the body decreases.

The structure of a fluidized bed near an immersed body differs substantially from that in an unperturbed part of the bed: the aerodynamic wake above the body has a stagnant zone with little circulation in the grains

All-Union Scientific-Research Institute of Agricultural Mechanization, Moscow.

Translated from Inzhenerno-Fizicheskii Zhurnal, Vol. 31, No. 5, pp. 807-814, November, 1976. Original article submitted November 14, 1975.

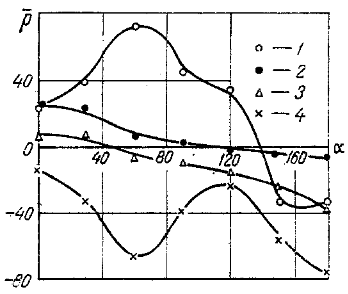

Fig. 1

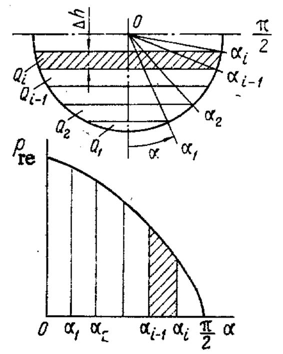

Fig. 2

Fig. 1. Distribution of the pressure coefficient around a sphere in a fluidized bed (N = 1.25): 1) d = 50 mm; 2) 30; 3) 90; 4) 70 mm; α, deg.

Fig. 2. Determination of the aerodynamic upthrust p_a; p_{re} is in Pa and α is in deg.

[1, 2, 5, 13], while under the lower half of the body there is a layer free from grains or else with a reduced grain concentration [5, 6, 9, 13]. We have found on observing the flow around a cylinder in a fluidized bed that a zone with little particle circulation is produced under the body at low fluidization numbers (forward stagnant zone). This observation agrees with the views presented in [10, 11].

A grain entering the free air layer around the lower half of the body is entrained by the flow and carried upward, which indicates that the flow speed around the body is higher than the mean speed in the gaps between the grains.

The speed differences between the unperturbed part of the bed, the free layer near the body, and in the forward and rear stagnant zones predetermine the pressure differences at a given level. Consequently, the pressure distribution over the body does not correspond to the linear distribution of the static pressure in a uniformly fluidized bed, so the upthrust should differ from the Archimedean value even if we neglect the force exerted by the upper stagnant zone.

The aerodynamic upthrust is a combination of the various forces arising from the fluidizing agent; the force from the flow around a sphere can be determined if the pressure distribution is known. The latter can be derived from data obtained with spheres of diameter 30, 50, 70, and 90 mm immersed in fluidized beds. Holes of diameter 0.2 mm were placed in the meridional plane at intervals of 30° between the forward critical point and the rear one, and were connected to a multichannel micromanometer. The connecting tubes of diameter 2 mm were brought out from the sphere on the side opposite to the holes and had no effect on the structure of the bed.

There was no change in the readings upon rotating the sphere around its vertical axis, so the pressure varies essentially in the vertical plane only.

The pressure distribution may be characterized via the dimensionless pressure coefficient $\bar{p}$, which is defined as the ratio of the difference between the pressure at the given point and the static pressure at infinity to the dynamic pressure for the unperturbed flow [4].

The flow around a sphere in an unbounded fluidized bed has an equivalent static pressure at infinity equal to the static pressure at the depth of the relevant point in the bed. The speed of the unperturbed flow is equal to the reduced speed. Then the pressure coefficient as defined above is

$$\bar{p} = \frac{p - p_s}{\frac{\rho V^2}{2}}. \tag{1}$$

The static pressure in the bed was determined with a multichannel alcohol micromanometer. The pressure was measured through lateral holes in blind tubes immersed in the bed.

The granular material was silica gel (d_e = 5.2 mm; ρ_g = 1740 kg/m^3). The tank had dimensions 0.35 × 0.36 m^2. The bottom was formed by a brass grid of cell size 0.1 mm, which was mounted as four layers to form a grid with an effective clear cross section of 0.4. Additional adjustable devices provided further equalization of the air flow.

The complete depth of the fluidized bed was in the range 116-142 mm as the fluidization number was varied over the range 1-3.6; the speed for onset of fluidization was 1.4 m/sec.

The pattern of air flow around an immersed sphere is almost the same as that for a sphere in a free air flow [4], although the sphere diameter does have some effect on the pressure distribution (Fig. 1), as do the air speed and the depth of immersion. The absolute values of these pressure coefficients, on the other hand, are much larger than those for an unbounded air flow, while the angles at which the positive values go over to negative ones vary widely. Sometimes there were no positive pressure coefficients.

The negative values are due to the ejection in the free layer around the body. The velocity around the sphere must be continuous, so it increases with the reduced flow speed and as the sphere diameter increases.

The magnitude and sign of the pressure coefficient are dependent on the thickness of the air layer. Photographs of cylinders showed that the thickness was greatest for a cylinder of diameter 50 mm. Figure 1 shows that the largest pressure coefficients occurred for a sphere of diameter 50 mm. The highest aerodynamic density occurred in the bed–sphere system also for a diameter of 50 mm. The relationship between layer thickness and the pressure at the surface occurred because the air speed is lower in a highly developed layer, so the ejection is less pronounced.

The pressure on the leading part of a sphere, especially a large one, is substantially affected by the leading stagnant zone. The pressure rise occurs because the increased aerodynamic resistance reduces the flow speed in this zone, so there is no ejection. Measurements showed that the regions of reduced or elevated pressure extended downward by 10-40 mm.

Immersion of the sphere in the bed to a depth of h = (1.1-1.3)d caused the absolute values of the pressure coefficients to increase; any further increase in the depth left them unchanged until the sphere reached the zone immediately above the grid, the exact distance varying from 10 mm for large spheres to 30 mm for small ones. The values for the pressure coefficients in this zone then tended to fall, because the porosity of the fluidized bed is reduced there, while near the body it tends to be elevated because of difficulty of access for grains displaced by the flow. As a result, the pressure coefficients deviate from the values for unbounded flows.

The integral aerodynamic upthrust was calculated by replacing the air flow by some equivalent fluid whose density varies with depth, which exerts a pressure equal to the pressure of the air in the fluidized bed. The treatment was simplified by referring pressure on the entire surface to the lower hemisphere by finding the pressure difference at diametrically opposite points in the lower and upper hemispheres. Then the lower hemisphere was split up into belts having central angles $\alpha_0-\alpha_1\ldots\alpha_i-\pi/2$ (Fig. 2). The graph for $p_{re} = f(\alpha)$ also splits up into the corresponding number of parts $\alpha_0-\alpha_1\ldots\alpha_i-\pi/2$, with $p_{re} = f(\alpha)$ within each part linear. This allows one to assume that the density of the equivalent liquid within each layer is constant at

$$\rho_{re\ i} = \frac{\Delta p_{re\ i}}{\Delta h_i} \tag{2}$$

whereupon the aerodynamic upthrust can be determined from the Archimedes principle. The integral aerodynamic upthrust on the whole sphere is

$$F_a = \sum_1^i \rho_{re\ i} Q_i. \tag{3}$$

The separating capacity of a fluidized bed may be deduced from the upthrust via the corresponding apparent densities; if the aerodynamic upthrust corresponds to the density of an equivalent liquid or to the apparent aerodynamic density of a fluidized bed, then the corresponding force is

$$F_a = \rho_a Qg. \tag{4}$$

Then (4) allows us to determine the apparent density of the equivalent liquid or the apparent aerodynamic density ρ_a of a fluidized bed.

The effective density is derived similarly in terms of the actual upthrust F_A; in the range of fluidization numbers used (N ≤ 1.36), the pressure fluctuations occur at high frequencies and have small amplitudes, so the fluctuations are of local character, in which case they make no major contribution to the upthrust, which is a difference from the situation at high N [8]. Therefore, the fluidization can be considered as homogeneous in this case.

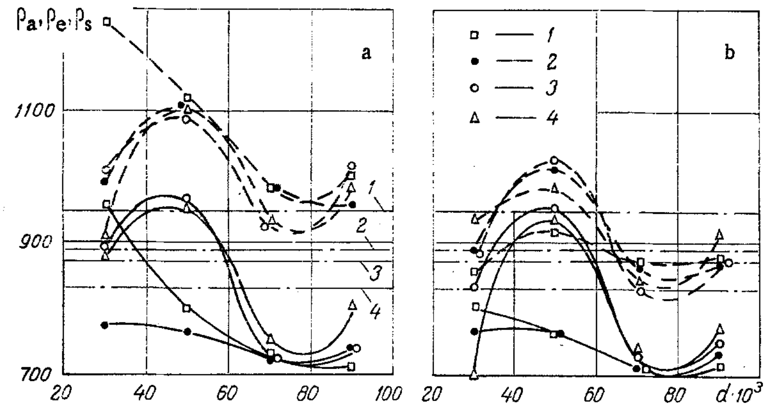

Fig. 3. Apparent aerodynamic density and effective density for a fluidized bed as a function of sphere diameter: a) (H − h) = 30 mm; b) h = d; dashed-dot line) density of suspension; dashed curve) apparent aerodynamic density of fluidized bed; solid curve) effective density [1) N = 1.03; 2) 1.18; 3) 1.25; 4) 1.36]. ρ_a, ρ_e, ρ_s, kg/m³.

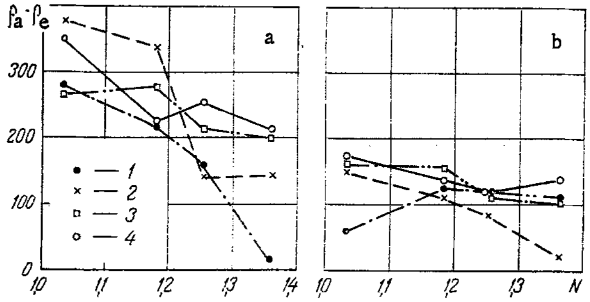

Fig. 4. Density difference $\rho_a - \rho_e$ as a function of the fluidization number: a) (H−h) = 30 mm; b) h = d; 1) d = 30 mm; 2) 50; 3) 70; 4) 90 mm; ρ_a, ρ_e, kg/m³.

We determined F_A by weighing the sphere in air and in the fluidized bed; the sphere was hung on a thin wire connected to an electrical balance, and the results served to define the effective density

$$\rho_e = \frac{F_A}{Qg}\ . \tag{5}$$

The density of the suspended grains is

$$\rho_s = \rho_g(1 - \varepsilon). \tag{6}$$

Figure 3 shows $\rho_a = f(d)$; $\rho_e = \psi(d)$ and ρ_s for various fluidization numbers as derived by experiment from (3)-(6).

The aerodynamic density was higher than that of the suspension and also above the effective bed density for spheres of diameter 30-90 mm with h > d. This occurs because F_a is greater than F_A on account of the effects mentioned above.

The effective density as a function of sphere size reproduces the behavior of the apparent aerodynamic density, which showed that the actual force (determined as the difference between the weight of the sphere in air and in the bed) is simply the aerodynamic upthrust reduced by some opposing force. The last consists of the weight of the granular material in the upper stagnant zone and the resistance of the fluidized bed to the movement of the latter. There is a ring of rising bubbles or air jets between this and the fluidized bed proper, so the frictional forces can be neglected in a first approximation. In that case, $\rho_a - \rho_e$ corresponds to the mass of grains in the upper stagnant zone as referred to the volume of the sphere, namely, the relative mass of the cap. Figure 4a shows that the relative mass of this cap increases with the diameter of the sphere.

The trend in ρ_a and ρ_e with sphere diameter is dependent on the fluidization number and immersion depth; if N is less than 1.18, which corresponds to incomplete fluidization, ρ_a and ρ_e decreases as d increases, which is followed by a minimum at d of 70-80 mm and then by a slight rise (except for ρ_a for h = d). If N exceeds 1.18, $\rho_a = f(d)$ and $\rho_e = \psi(d)$ have a second turning point at d = 40-50 mm.

The effective density may thus be higher or lower than the density of the suspension, the size of the sphere being the decisive factor. The effective size of the sphere, namely, the size at which the effective density equals that of the suspension, increases with the fluidization number, but there is a certain range in N in which the effective density is less than the suspension density for all sphere sizes.

The rear stagnant zone is filled with largely immobile grains only if the sphere is fairly deep within the bed, so one expects that the effective density would be higher with the sphere only partly immersed. However, parts a and b of Fig. 3 show that the effective density is actually less (if h = d, when there are virtually no suspended grains resting on the sphere) than it is for deep immersion. Since the air layer around the sphere lies near the free surface of the bed, there is a marked reduction in the resistance to the bubbles or jets, which reduces the aerodynamic upthrust on the body.

The difference between the apparent aerodynamic density and the effective density is much less if the sphere lies near the surface, and the difference is less dependent on the fluidization number (Fig. 4b).

The effective density above the grid is reduced for small spheres, as would be expected, since the pressure coefficients in this region are somewhat less.

The structure of the fluidized bed near the body, together with the pressure distribution and the similarity of the $\rho_a = f(d)$ and $\rho_e = \psi(d)$ curves, indicates that the hydrodynamic setting around a body is due to interaction between two types of flow; hindered flow around the body and the main flow passing through the unperturbed part of the bed. The ultimate result is determined by the characteristics of both flows, and these themselves are dependent on the properties of the fluidized material, the size of the body, the fluidization speed, the distance of the body from the distributing grid, and the distance from the surface of the bed.

NOTATION

d	is the sphere diameter, m;
d_e	is the equivalent diameter of grains, m;
F_a	is the integral aerodynamic buoyancy force, N;
F_A	is the Archimedean upthrust; N;
g	is the acceleration due to gravity, m/sec^2;
H	is the total depth of fluidized bed, m;
h	is the depth of bottom of sphere , m;
Δh_i	is the height of sphere bed, m;
p	is the air pressure at sphere surface, Pa;
$\bar{p}$	is the pressure coefficient;
p_{re}	is the surface pressure referred to the lower hemisphere, Pa;
Δp_{rei}	is the pressure drop in bed in sphere section, Pa;
Q	is the sphere volume, m^3;
Q_i	is the volume of sphere bed, m^3;
V	is the fluidization speed referred to the area of the unloaded section, m/sec;
V_0	is the initial fluidization speed, m/sec;
$N = V/V_0$	is the fluidization number;
α	is the flow angle for sphere, deg;
ε	is the porosity;
ρ	is the density of air, kg/m^3;
ρ_a	is the apparent aerodynamic density of fluidized bed, kg/m^3;
ρ_s	is the density of solid suspension, kg/m^3;
ρ_e	is the effective density of fluidized bed, kg/m^3;
ρ_{rei}	is the density of equivalent liquid for sphere bed, kg/m^3;
ρ_g	is the density of grains, kg/m^3;

LITERATURE CITED

1. A. P. Baskakov, B. V. Berg, and V. V. Khoroshavtsev, Teor. Osn. Khim. Tekhnol., 5, No. 6 (1971).
2. V. I. Buryakov, Author's Abstract of Candidate's Dissertation, Karaganda (1968).

3. V. P. Gupalo, Inzh.-Fiz. Zh., 5, No. 2 (1962).
4. M. E. Deich, Engineering Gasdynamics [in Russian], Moscow–Leningrad (1961), pp. 79, 289.
5. Yu. I. Zinov'ev, Vestn. S.-Kh. Nauki, No. 11 (1959).
6. V. N. Korolev and N. I. Syromyatnikov, Tr. Ural'sk Politekh. Inst., No. 205, 133 (1972).
7. M. L. Liberman, A. A. Pikhlak, and Yu. A. Groshev, in: Papers from the Central Informatics and Economics Research Institute of the Coal Industry, No. 5. Dressing and Briquetting of Coal [in Russian] (1962).
8. B. A. Michkovskii and A. P. Baskakov, in: Heat and Mass Transfer and the Nonequilibrium Thermodynamics of Disperse Systems [in Russian], UPI, Sverdlovsk (1974).
9. N. I. Syromyatnikov and V. M. Kulikov, Inzh.-Fiz. Zh., 23, No. 6 (1972).
10. G. P. Cherepanov, Zh. Prikl. Mekh. Tekh. Fiz., No. 6 (1966).
11. D. N. Allen, Quart. J. Mech. Appl. Math., 2, Pt. 1 (1949).
12. T. C. Daniels, J. Mech. Eng. Sci., 4, No. 2 (1962).
13. D. H. Glass and D. Harrison, Chem. Eng. Sci., 19, No. 12 (1964).
14. H. Reuter, Chem.-Ing.-Tech., 38, No. 8 (1966).

HYDRAULIC RESISTANCE AND HEAT TRANSFER IN A PULSATING FLOW OF A GAS–SOLID MIXTURE

V. V. Mamaev, V. S. Nosov,
and N. I. Syromyatnikov

UDC 536.244:532.582.7

It is shown that the heat-transfer coefficient can be increased by 30-35% if periodic fluctuations in speed occur in an ascending gas–solid mixture.

Much importance has recently been attached [1] to pulsed pneumatic transport, in which there is a strictly periodic air input into a pipeline. This provides similar speeds for the carrying medium and bunches of material, which provide for considerably improved range and performance.

On the other hand, forced velocity pulsation superimposed on a uniform flow may accelerate heat transfer [2, 3], while colliding jets of suspensions and pulsations in ascending gas–solid flows at resonance may accelerate heat transfer between phases [4].

Here we report measurements on velocity pulsations and heat transfer for gas–solid suspensions in pipes.

The equipment has previously been described [5]; the velocity fluctuations were produced by periodically altering the cross section of the pipe before or after the working section, which was a steel tube of internal diameter 8 mm and length 800 mm. The pulsation frequency was in the range 1-12 Hz and was recorded by a clock system (1 Hz) or by a stroboscopic tachometer (5 or 12 Hz). The amplitude of the pulsations in the flow rate was estimated from the fluctuations in the stagnation pressure. The Reynolds number varied in the range $(2\text{-}8.2)\cdot 10^3$, while the corresponding gas speeds were 4.6-17.5 m/sec. The electrocorundum particles of diameter 60 μ were used at concentrations from 0 to 11 kg/kg. The value did not exceed 6 kg/kg at low gas speeds.

The time-averaged pressure difference over the working section was measured with a micromanometer.

The studies amounted to determining the empirical factor K applicable to the resistance due to the particles in the flow.

The definition of K is as follows [6]:

Kirov Urals Polytechnic Institute, Sverdlovsk. Translated from Inzhenerno-Fizicheskii Zhurnal, Vol. 31, No. 5, pp. 815-820, November, 1976. Original article submitted October 13, 1975.